Formation and characterization of nanotubes of $La(OH)_3$ obtained using porous alumina membranes

2008 Nanotechnology 19 495305

(http://iopscience.iop.org/0957-4484/19/49/495305)

Nanotechnology **19** (2008) 495305 (9pp) doi:10.1088/0957-4484/19/49/495305

Formation and characterization of nanotubes of $La(OH)_3$ obtained using porous alumina membranes

L González-Rovira[1], J M Sánchez-Amaya[1], M López-Haro[2], A B Hungria[2], Z Boukha[3], S Bernal[3] and F J Botana[1]

[1] Departamento de Ciencia de Materiales e Ingeniería Metalúrgica y Química Inorgánica, Laboratorio de Ensayos, Corrosión y Protección, Universidad de Cádiz, Lab. 712, CASEM, Avenida República Saharaui s/n, Puerto Real, E-11510 Cádiz, Spain
[2] Departamento de Ciencia de Materiales e Ingeniería Metalúrgica y Química Inorgánica, Grupo de Estructura y Química de Nanomateriales, Universidad de Cádiz, Facultad de Ciencias, Avenida República Saharaui s/n, Puerto Real, E-11510 Cádiz, Spain
[3] Departamento de Ciencia de Materiales e Ingeniería Metalúrgica y Química Inorgánica, Grupo de Química de Sólidos y Catálisis, Universidad de Cádiz, Facultad de Ciencias, Avenida República Saharaui s/n, Puerto Real, E-11510 Cádiz, Spain

E-mail: javier.botana@uca.es

Received 25 July 2008, in final form 22 October 2008
Published 18 November 2008
Online at stacks.iop.org/Nano/19/495305

Abstract
An electrodeposition process is used to synthesize nanotubes of a lanthanum-containing phase, employing porous alumina membranes as templates. This method should lead to the formation of $La(OH)_3$ nanowires, according to the previous results presented by Bocchetta *et al* (2007 *Electrochem. Commun.* **9** 683–8), which can be decomposed to La_2O_3, as the latter shows more interest for different applications. The results obtained by means of different electron microscopy techniques indicate that this method leads to the formation of nanotubes of about 200 nm in diameter and 30–40 μm in length, instead of the nanowires proposed in the literature. Additionally, the chemical characterization demonstrates that the material synthesized is composed of lanthanum hydroxycarbonate. The presence of carbonates is found to be crucial in determining the conditions for the preparation of La_2O_3 from the nanotubes here obtained.

1. Introduction

There has been growing interest in the study of nanomaterials in recent years due to their potential applications in many different areas of science and technology. Particular attention has been given to the design of methods for the formation of nanostructured materials such as nanowires, nanotubes, nanobelts and nanorods. Nanostructures of these types have become essential in the design of catalysts, sensors and others devices [2–7].

One of the methods proposed in the bibliography for the formation of different types of nanomaterials is to utilize porous alumina membranes as templates. This method has been successfully employed in the synthesis of nanowires and nanotubes from compounds of very diverse natures and applications (metals, semiconductors, polymers) [1, 8–12]. However, very few studies have been reported in which this method has been utilized to prepare oxides or hydroxides with applications in catalysis [1, 13, 14].

The present study deals with the preparation of Al_2O_3/La_2O_3 catalytic systems with potential use in the synthesis of biodiesel. In this system, La_2O_3 is the species that presents the catalytic activity due to its basic character, while the alumina, in the form of porous anodic membranes, fulfils a structural role. However, it is practically impossible to incorporate the lanthanum in the interior of the pores by using conventional impregnation methods [15, 16]. For this reason, an alternative method is proposed consisting of electrodeposition treatments, carried out with solutions of lanthanum salts, by means of which the lanthanide compound gets incorporated into the porous structure of the alumina.

A method to obtain nanowires of $La(OH)_3$ and $Nd(OH)_3$ is described in [1]. This method is based on an

electrodeposition process using $La(NO_3)_3$ or $Nd(NO_3)_3$ solutions and commercially available membranes of porous alumina as templates. The authors characterize the materials obtained by scanning electron microscopy (SEM), energy-dispersive x-ray spectrometry (EDS) and x-ray diffraction measurements. This characterization leads them to conclude that the hydroxide of the element employed can be obtained in the form of dense, continuous and defect-free nanowires. In addition, these authors propose transforming the $La(OH)_3$ by thermal decomposition into La_2O_3, which has more applications than $La(OH)_3$. Although the temperature of decomposition of the hydroxide is a critical parameter for the synthesis of the oxide, it is not studied in [1].

In the present work, the methodology described in [1] to obtain nanowires of $La(OH)_3$ has been initially followed, with the main objective of improving the characterization work, making use of a wider range of experimental techniques. The results indicate that, contrary to the conclusion reached in [1], the procedure utilized produces nanotubes instead of nanowires, containing the obtained phase lanthanum hydroxycarbonate. The nanotube morphology, together with its carbonated nature, will condition the behaviour of these compounds for different applications and, at the same time, will determine the conditions necessary for preparation of the La_2O_3 [17].

2. Experimental details

Commercial membranes of anodic alumina, 60 μm thick and with pore diameters of approximately 200 nm, were employed. In order to facilitate the electrodeposition, a fine layer of gold was deposited on one of the faces of these membranes. It was confirmed that the layer of gold deposited did not plug the pores of the face treated. This treatment allows the membrane to be utilized as the cathode of a cell of three electrodes used in the process of electrodeposition. The electrical contact with the membrane is made by a copper plate on which the metallized face of the membrane is seated. The surface area of sample exposed to the solution is 1 cm^2. A net of platinum wires is utilized as the auxiliary electrode, and one of Ag/AgCl 3 M is employed as a reference electrode. The electrodeposition was performed for a period of one hour in a solution of $La(NO_3)_3$ 0.05 M at ambient temperature in the galvanostatic regime, applying 1 mA cm^{-2}.

Once the material was prepared the nanotubes were separated from the alumina template. Firstly, the film of gold was dissolved by immersing the samples in a solution of I_2 6 mM and KI 6 mM in ethanol for a period of 30 min at room temperature. Secondly, the template of alumina was dissolved by immersion in an aqueous solution of NaOH 1 M at 45 °C for 3 h. Finally, the resulting solid product was rinsed with ethanol and characterized morphologically and chemically using various experimental techniques.

The morphological study was performed by scanning electron microscopy (SEM), scanning transmission electron microscopy in high angle annular dark-field mode (STEM-HAADF) and high resolution electron microscopy (HREM). The chemical characterization was performed using energy-dispersive x-ray spectrometer (EDS), Fourier-transform infrared spectroscopy (FTIR), thermogravimetric analysis (TGA), programmed thermal desorption coupled to mass spectrometry (PTD-MS) and x-ray diffraction (XRD).

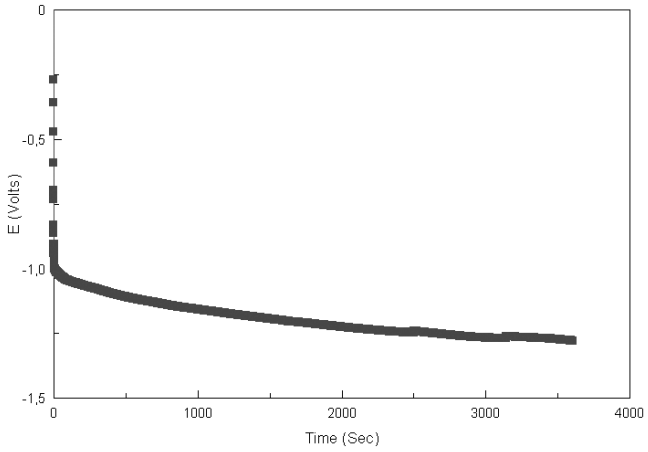

Figure 1. Variation of the potential as a function of time during the electrodeposition of $La(OH)_3$ at 1 mA cm^{-2}.

3. Results and discussion

3.1. Synthesis of the nanotubes of La(OH)$_3$

The process for obtaining the nanowires proposed in [1] is based on precipitating $La(OH)_3$ from $La(NO_3)_3$ solutions. According to [1, 18], when this solution is cathodically polarized the reduction of the nitrate ions occurs in accordance with equation (1):

$$NO_3^- + H_2O + 2e^- \rightarrow NO_2^- + 2OH^-. \quad (1)$$

The employed experimental set-up allows the reduction of the solution inside the pores of the alumina template. Reaction (1) provokes a local increase of the pH, reaching the required conditions for the precipitation reaction of $La(OH)_3$, in accordance with equation (2):

$$La^{3+} + 3OH^- \rightarrow La(OH)_3 \downarrow . \quad (2)$$

Most of the electrodeposition experiments have been performed in the galvanostatic regime, applying 1 mA cm^{-2}. In figure 1 the variation of the potential during this process is represented. It can be appreciated in figure 1 that the potential of the system increases in absolute terms with the time of electrodeposition, which demonstrates that the resistance in the system is increasing. This increase in the resistance can be attributed to the precipitation of $La(OH)_3$ in the interior of the pores.

3.2. Morphological characterization of the nanotubes of La(OH)$_3$

Figure 2(a) includes an SEM image of the obtained material after the electrodeposition process and once the alumina

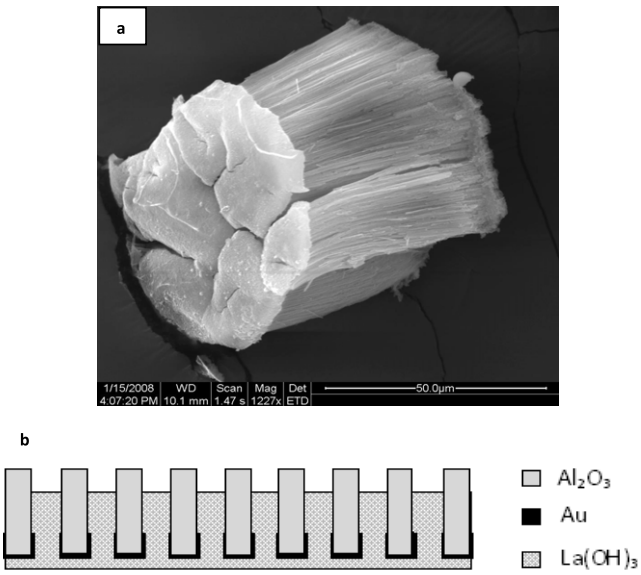

Figure 2. (a) SEM image of the material obtained after dissolving the alumina membrane. (b) Diagram of the $Al_2O_3/La(OH)_3$ system formed after the electrodeposition.

membrane has been dissolved. This figure shows that this material presents two zones with different morphologies. Thus the existence of cylindrical wires, arranged in parallel, can be observed (right side of figure 2(a)). It can also be observed that these wires are held, at their base, by a layer of more compact appearance and of irregular thickness (left side of figure 2(a)). In accordance with the diagram proposed in figure 2(b), the layer to which the wires are fastened can be attributed to the hydroxide precipitated outside the pores, on the membrane base, while the wires themselves would be formed by the precipitation inside the pores.

Figure 3 includes SEM images of the same sample of figure 2, obtained at different magnifications. From the images taken at low magnification, figures 3(a) and (b), it seems that, as proposed in [1], the materials obtained are compact, continuous and defect-free 'nanowires'. According to the images in figures 3(a) and (b), it could be thought that these structures are 'nanowires' with a diameter of around 200 nm (nominal diameter of the pores of the template) and a length of 30–40 μm. However, the SEM images acquired at greater magnification, figures 3(c) and (d), suggest that the obtained structures present hollow regions inside them, that is, they are nanotubes instead of nanowires. With the object of making a more detailed characterization of their microstructure, further studies were performed by means of STEM-HAADF. The images obtained using this technique are included in figures 4 and 5. At this point, it is necessary to emphasize that the contrast seen in the STEM-HAADF images may be due to variations in the thickness of the material (in samples of a homogeneous composition) or to variations in the mean atomic number (in samples of equal thickness). Since the X-EDS analysis performed on the obtained samples indicates a uniform composition, it can be concluded that the variations in contrast observed in the STEM images of figure 4 should be interpreted as a consequence of different thicknesses. In these images, the higher the intensity, the higher the thickness of the

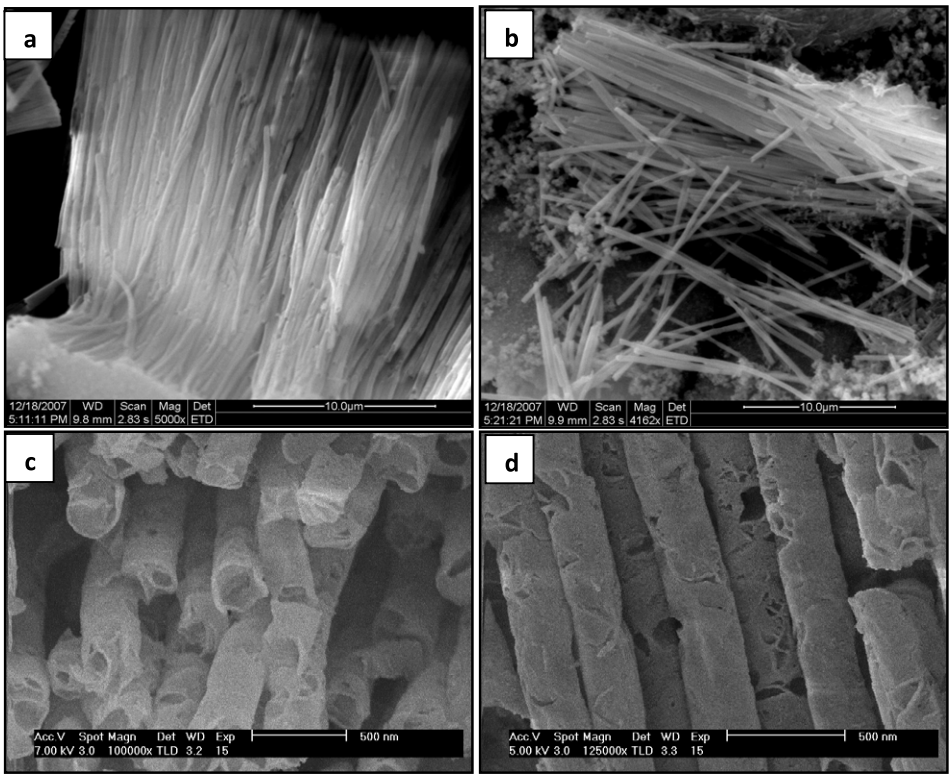

Figure 3. SEM images at low ((a) and (b)) and at high ((c) and (d)) magnification of the $La(OH)_3$ nanotubes after elimination of the alumina membrane.

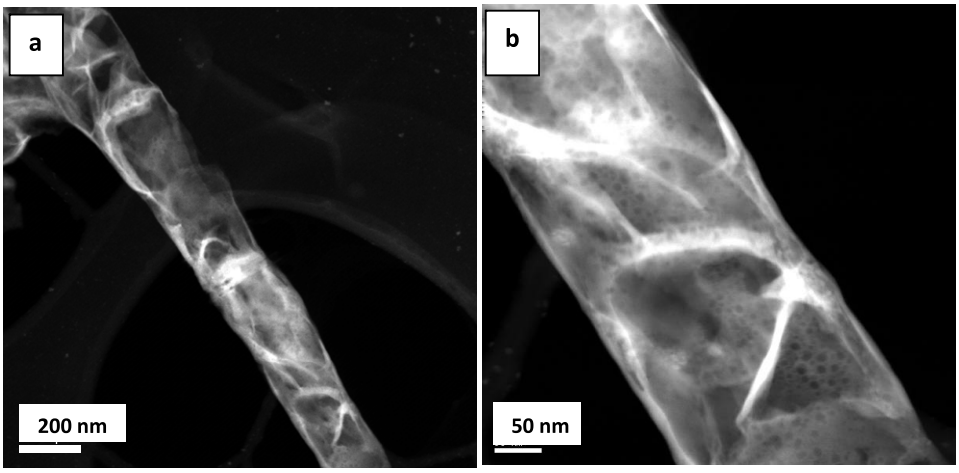

Figure 4. STEM-HAADF images of the $La(OH)_3$ nanotubes after being extracted from the alumina membrane.

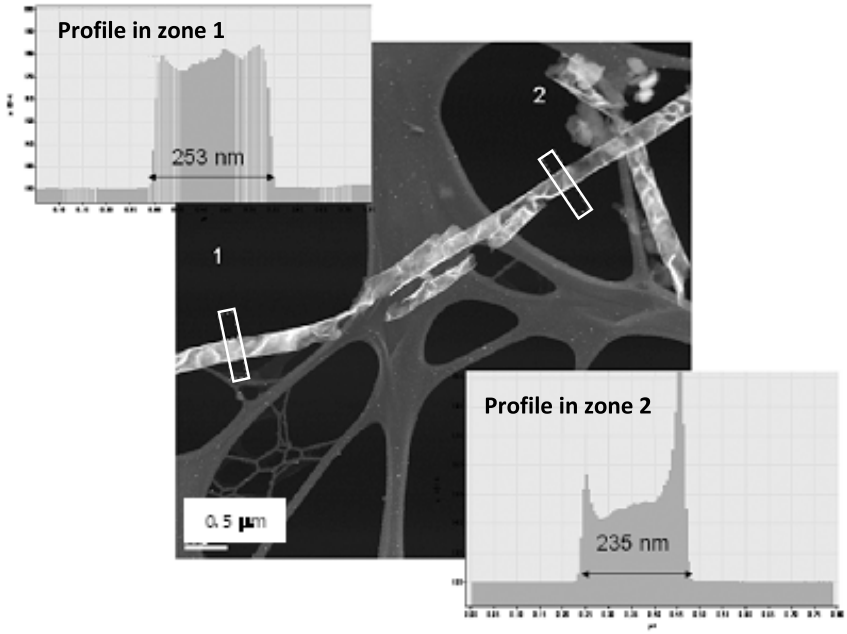

Figure 5. Measurements of the diameter of a tube of $La(OH)_3$ made on the intensity profiles in a STEM-HAADF image.

region. As can be noticed in figure 4, the edges (external zones) of the structures are brighter than the central parts (internal zones). This confirms that the structures are hollow, being nanotubes rather than nanowires.

In the image recorded at greater magnification, figure 4(b), details of the internal structure of the nanotubes can be observed. In this figure it is possible to observe rounded regions of low intensity, with diameters of the order of one nanometre. These contrasts can be attributed to the existence of small pores in the walls of the tubes. It is thought that the origin of these pores could be due to hydrogen bubbles that evolved on the cathodic sites during the process of electrodeposition. It can also be appreciated in figure 4(b) the presence of narrow and curved bands of high intensity. The existence of these contrasts may be due to cracks of the nanotubes in these zones of the surface. In these regions, the wall of the tube is folded over on itself, giving these high intensity bands in the STEM-HAADF images. These results are in agreement with those obtained from the SEM images of high magnification, figure 3(d), where the presence of folds and apertures can be confirmed.

From the STEM-HAADF images, intensity profiles can be acquired along the transversal section of the nanotubes, figure 5. These profiles have been used to estimate diameters of the nanotubes, an average value of 245 nm having been measured. Some of the tubes presented diameters of up to 253 nm, figure 5. It should be recalled, on this point, that the membranes utilized as templates have a nominal pore diameter of the order of 200 nm. Thus the forms appear to have a diameter around 20% larger than that of the pores of the membrane in which they were grown. This fact can be explained if the structures are considered hollow nanotubes

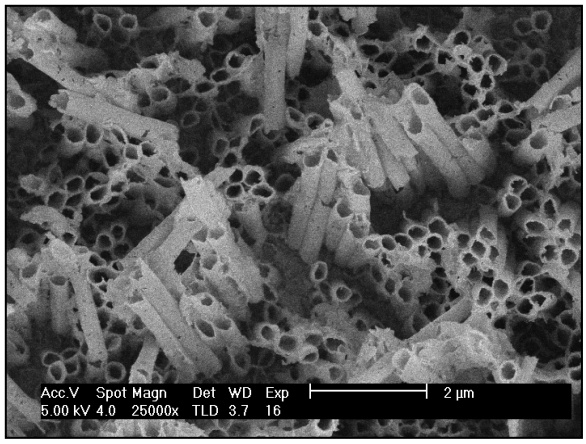

Figure 6. SEM image of nanotubes of $La(OH)_3$ formed in a 0.01 M solution of $La(NO)_3$ applying 1 mA cm^{-2} after being extracted from the alumina membrane.

whose walls are not rigid enough, so when the nanotubes are extracted from the alumina matrix, the structure of the tube may distort to a certain degree. This process would give rise to a flattened nanotube. This structure would have a diameter larger than those of the pores of the alumina membrane.

The influence of the concentration of lanthanum nitrate in the solution on the formation processes of nanotubes has been analysed by performing another series of electrodeposition experiments. Figure 6 is an SEM image of the material grown utilizing a 0.01 M solution of $La(NO_3)_3$ applying a constant current of 1 mA cm^{-2} for 1 h. When comparing the nanotubes formed in 0.01 M $La(NO_3)_3$ solution (figure 6) with those in 0.05 M (figure 3), it can be stated that, although the diameter is similar in both conditions because of the same pore size, the length and wall thickness seem different. Thus, increasing the concentration of $La(NO_3)_3$ has the effect of increasing the length of the nanotubes and, to a lower extent, also their wall thickness.

It could be checked that the tubes grown in 0.05 M solution were not transparent to electrons, so it was impossible to record HREM images from these samples. However, HREM images of the nanotubes grown in 0.01 M solution could be obtained. It confirms that the walls of the nanotubes formed in the 0.01 M solution are thinner than those formed in the 0.05 M solution. This reveals that the wall thickness of the nanotubes decreases when the concentration of the solution utilized for electrodeposition is decreased. Figure 7 shows representative HREM images corresponding to two different zones of the tubes obtained in the 0.01 M solution. Figure 7(a) shows a region corresponding to the internal zones of the tube, that is, the central zone which is more distant from the wall of the nanopore in which the tube had formed. The image in figure 7(c) corresponds to more superficial regions of the tubes,

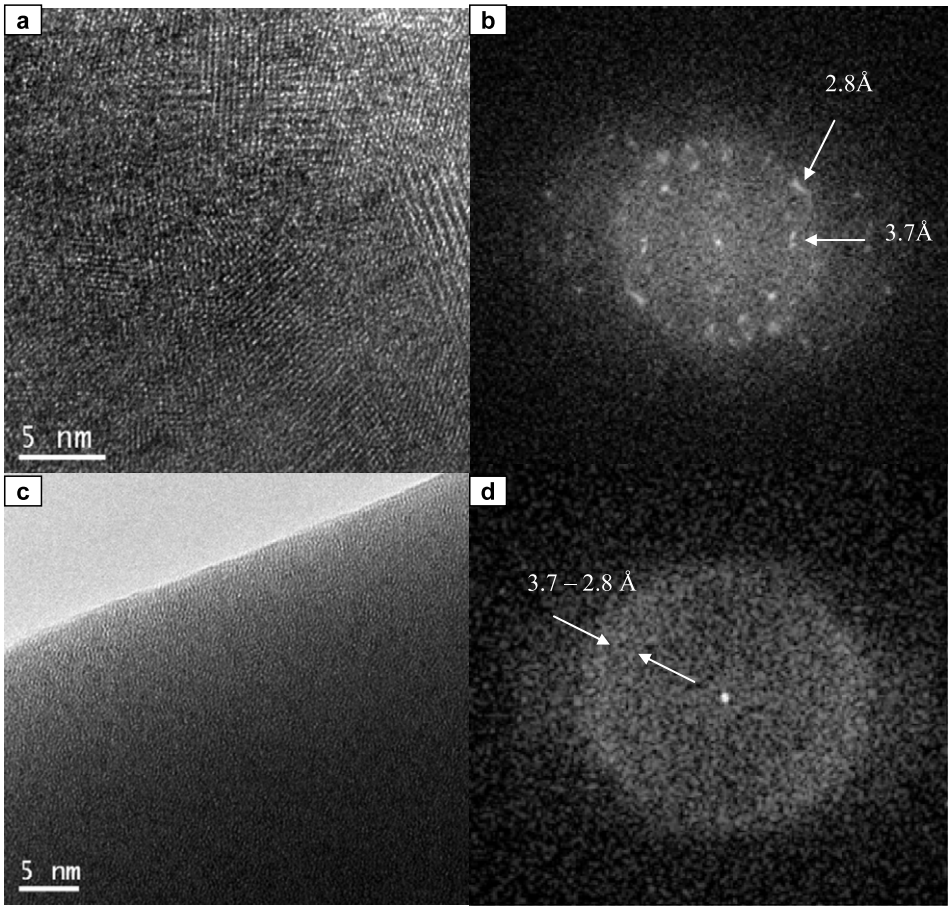

Figure 7. HREM images of the (a) interior and (c) exterior zone of the wall of a nanotube formed in $La(NO_3)_3$ 0.01 M applying 1 mA cm^{-2} for a period of 1 h; (c) and (d) digital diffraction pattern (DDP) corresponding to each HREM image on the left.

that is, to the zones of contact with the walls of the nanopores. Figures 7(b) and (d) show, in the form of a digital diffraction pattern (DDP), the results of the analysis of these images by Fourier transform.

Although differences in the nature of the contrasts between the two zones can be appreciated in figure 7, in all cases the images and their corresponding diffractograms indicate that the tube is of crystalline nature, in both the more external and the internal regions. In the images recorded of the more internal zones (figures 7(a) and (b)), interplanar spacings can be clearly observed, extending in different directions. The diffractograms corresponding to these regions, in figure 7(b), indicate the systematic presence of reticular spacings of 3.7 and 2.8 Å. These are the spacings characteristic of the {102} and {202} planes of $LaOHCO_3$, respectively [19]. It is therefore evident, from inspection of both the HREM image and the DDP, that the tube is formed by agglomeration of a large number of crystalline domains, apparently disorientated with respect to each other, of this hydroxycarbonated phase. It should be noted that there are many reflections, in different relative orientations, in the zone of interplanar spacings mentioned. Similarly the existence of crystallites in very diverse orientations can be appreciated in the original HREM image.

With reference to the image of the zones at the edges of the tubes, figure 7(c), although a first visual inspection would suggest that the material in these regions is amorphous in nature, the diffractograms corresponding to these regions clearly indicate the presence of defined reticular spacings, figure 7(d). These diffractograms show specifically a ring of reflections ranging between 3.7 and 2.8 Å, the same spacings observed as predominant in the images of the interior of the tubes. This result indicates that, in this zone of the tubes, there are also crystals of the hydroxycarbonate phase, but of much smaller characteristic size. The superposition of a large number of these crystals, in different orientations along the direction of incidence of the electron beam, would be responsible for the peculiar appearance of the HREM images acquired in these regions.

In short, the above results confirm directly the formation of a hydroxycarbonate crystalline phase in the conditions of growth of the tubes. They also suggest that the crystal size of this phase tends to increase towards the interior of the tube, which is almost certainly the result of the 'seeding' effect caused by the first crystals that are deposited in direct contact with the walls of the nanopore.

Taking into account all the results discussed in this part, it can be concluded that the method described can be used to obtain nanotubes of a hydroxycarbonate crystalline phase, whose length and wall thickness depend on the experimental conditions employed during the deposition process.

3.3. Chemical characterization of the nanotubes of $La(OH)_3$

As stated in [17, 20], it is complicated to synthesize pure lanthanide hydroxides by means of conventional methods of synthesis. The root of this difficulty is that lanthanide hydroxides in contact with air react easily with atmospheric CO_2, giving rise to carbonated phases, a process so-called carbonatation. As a result, when these hydroxides are prepared, particularly of the first elements of the lanthanide series, it is usual to obtain non-stoichiometric carbonated phases and even hydroxycarbonate compounds. This behaviour described for massive hydroxides has not been described to date for nanostructured phases. In [1] no evidence of such kinds of processes is reported.

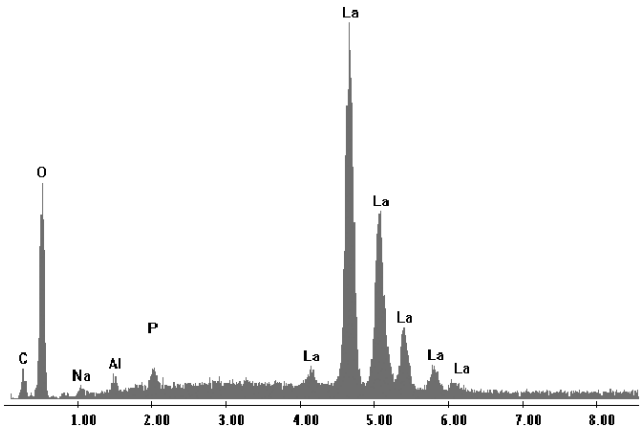

Figure 8. EDS spectrum of a sample of nanotubes obtained after electrodeposition and subsequent elimination of the alumina template.

As is commented bellow, the existence of carbonates in the samples has notable importance. In [1], it has been commented that one possible application for nanowires of $La(OH)_3$ is their utilization as precursors to obtain nanostructured La_2O_3, since there are many more applications for the oxide than for the corresponding hydroxide. The synthesis of nanostructured La_2O_3 would be carried out by thermal decomposition of the nanotubes of $La(OH)_3$ prepared as described in the present paper. If one wants to make use of this synthesis route, it is necessary to determine precisely the temperature of decomposition of the precursor, since the existence of carbonates means that a much higher temperature is necessary to generate pure La_2O_3 than if the precursor were pure $La(OH)_3$ [17, 21, 22].

The chemical characterization of the obtained nanotubes has been performed using x-ray energy-dispersive spectroscopy (EDS), thermogravimetric analysis (TGA), programmed thermal desorption coupled to mass spectrometry (PTD-MS) and FTIR spectroscopy.

The EDS spectrum included in figure 8 demonstrates that the nanotubes are mainly constituted of lanthanum and oxygen. The detection of peaks assignable to aluminium and phosphorus is due to the presence of remains of the alumina membrane in the sample analysed. Phosphorus is present because the membrane production process includes the anodization in a phosphoric acid solution. Also found are small quantities of sodium, originating from the solution of NaOH utilized to dissolve the alumina membrane after deposition. Finally, the existence of the signal corresponding to carbon originates from the carbon layer deposited in order to facilitate observation under the microscope and probably by the presence of carbonates.

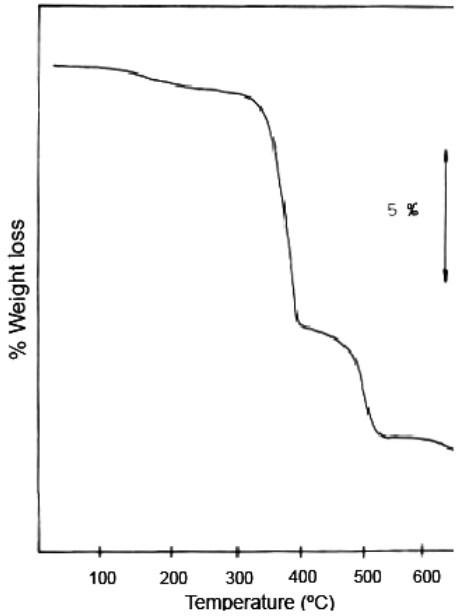

Figure 9. TGA diagram of a sample of $La(OH)_3$. Adapted from [17].

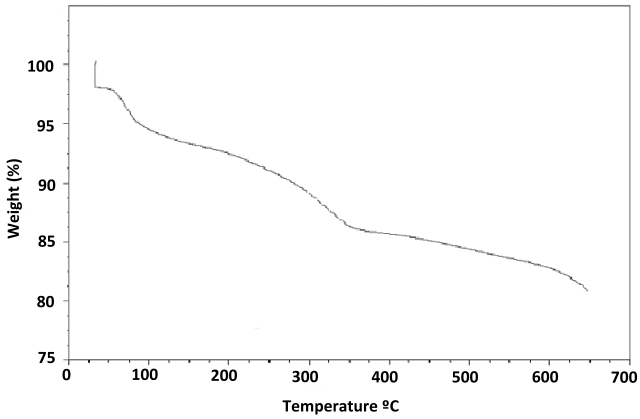

Figure 10. TGA diagram of a sample of nanotubes after elimination of the alumina template.

Table 1. Position and relative intensity values of the main peaks both in the experimental diagram and in the hexagonal $La(OH)_3$ ICDD card 36-1481.

ICDD card 36-1481 ($La(OH)_3$)			Experimental	
2θ	I	hkl	2Θ	I
15.67	60	100	—	—
27.30	62	110	26.84	100
27.97	100	101	—	—
39.48	75	201	—	—
47.06	13	002	47.56	82
48.265	38	300	—	—
48.6	61	211	—	—
55.3	21	112	55.68	31
56.312	10	220	—	—
75.800	8	103	75.88	30

According to [17, 21, 22], if the starting product is $La(OH)_3$, its thermal decomposition should take place in two clearly differentiated stages, with a ratio of 2:1 between the weight lost in the first and second stages. The TGA diagram for this type of sample should be similar to that shown as figure 9. Thus La_2O_3 should be obtained by calcining the hydroxide at around 500 °C.

Figure 10 shows the TGA diagram for the nanotubes obtained in this study. By comparing the diagrams in figures 9 and 10, it can be deduced that the product obtained must be different from $La(OH)_3$ since its TGA diagram is clearly different from that shown as figure 9. According to figure 10 it is necessary to heat the samples up to 850 °C to obtain pure La_2O_3.

In order to determine the chemical nature of the products generated during the thermal decomposition of the sample, PTD-MS experiments were performed. In figure 11 it can be seen that the thermal decomposition of the samples starts with the loss of water; peaks at low temperature can be observed in the diagrams of the signals with m/c ratios of 18, 17 and 16. In addition, in the PTD diagrams the presence of peaks at high temperature corresponding to the loss of CO_2 ($m/c = 44$) can be observed. In accordance with [16], these peaks are associated with the decomposition of the carbonated phases formed during the process of preparation of the samples. Therefore these results, together with those obtained by TGA, demonstrate that the nanotubes prepared present a high level of carbonatation.

The existence of carbonate groups can also be detected in the FTIR spectra of the nanotubes obtained, as shown in figure 12. In these spectra, the band that appears at 3605 cm^{-1} could be attributed to the tension of hydroxyl groups of lanthanide hydroxides [17, 22]. Another important band appears at 3430 cm^{-1} which is associated with hydroxyl groups of molecular H_2O. In lanthanide hydroxides the band at 3605 cm^{-1} is usually much more intense than the band at around 3430 cm^{-1}. However, in the spectrum shown in figure 12 there can be seen an inversion of the intensities between these bands, attributed by some authors to the existence of hydroxycarbonate-type $La(OH)CO_3$ with ancylite-type structure [17, 19, 23]. The carbonatation of the samples is also confirmed by the emergence of peaks at 866, 1055, 1460 and around 1396 cm^{-1}, which are characteristic of the normal vibration modes of lanthanide carbonates [17, 22].

Figure 13 shows the XRD diagram corresponding to an AAO membrane containing lanthanum nanotubes within its pores. Four well-defined peaks, with 2θ values of 26.84°, 47.56°, 55.68° and 75.88°, can be identified in this diagram. Table 1 summarizes position and intensity values of the main peaks both in the experimental diagram and in the hexagonal $La(OH)_3$ ICDD card 36-1481. When analysing data in table 1 it was noted that there is a substantial deviation of the relative intensities of the main reflections from those anticipated in the powder XRD standard. According to [24], changes in the relative intensity of the peaks can be due, when using AAOs as templates, to the formation of textured samples in which crystals grow along preferential directions. These results, similar to those reported in [1], suggest that $La(OH)_3$ nanotubes are formed by crystals grown, mainly along the (1, 1, 0) and (0, 0, 2) directions. Thus, the XRD diagram shown in figure 1 allows us to conclude that

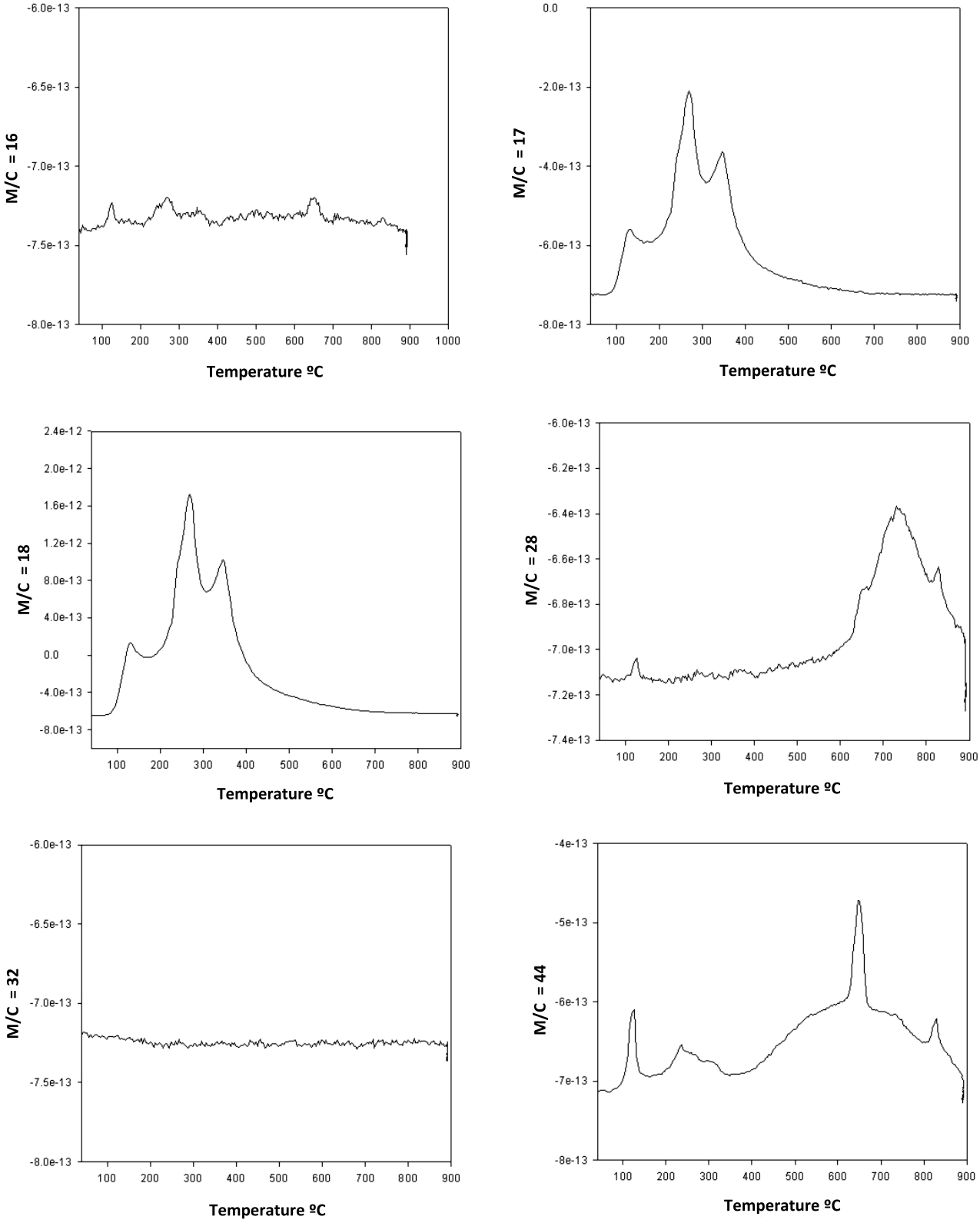

Figure 11. TPD-MS diagrams of a sample of nanotubes after the elimination of the alumina template.

the synthesized nanotubes are formed by highly textured $La(OH)_3$. Carbonation of the samples, detected by means of other characterization techniques, cannot be found using XRD, probably due to the tiny size of crystals in the carbonated phases.

In summary, the chemical characterization carried out, together with the data obtained by HREM, demonstrates that the method proposed in [1] enables nanotubes of a lanthanum hydroxycarbonate to be generated. The carbonatation of the sample has a big influence if the intention is to utilize these

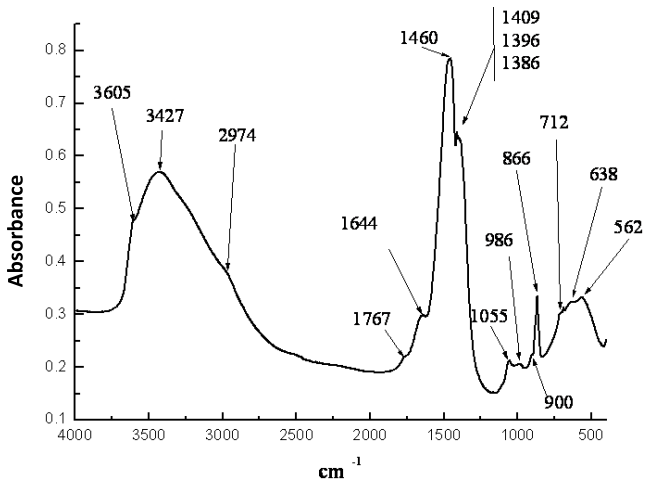

Figure 12. FTIR spectrum of the nanotubes obtained after the electrodeposition and subsequent elimination of the alumina template.

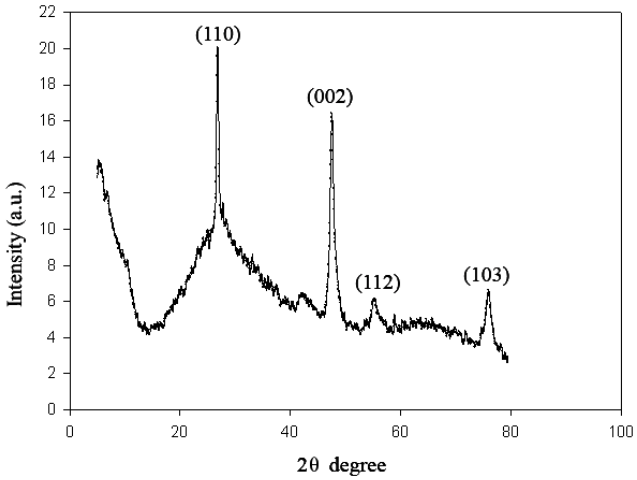

Figure 13. XRD diagram of the nanotubes obtained after the electrodeposition.

nanotubes as precursors in the preparation of La_2O_3, which has more applications than the hydroxide or related phases. In accordance with the data obtained in this study, to be able to obtain La_2O_3 free from carbonates it would be necessary to calcine the samples at temperatures of the order of 850 °C. By calcining the nanotubes at temperatures lower than that cited, carbonated phases would be obtained with chemical properties clearly different from those of La_2O_3.

4. Conclusions

A characterization study of the nanostructures obtained by electroreduction of an $La(NO_3)_3$ solution inside the pores of an alumina membrane has been carried out. According to [1], this method is reported to lead to the formation of $La(OH)_3$ nanowires. However, the morphological characterization results obtained using SEM, HAADF-STEM and HREM state that this method allows us to obtain nanotubes, instead of the nanowires proposed in the literature. Nanotubes are approximately 200 nm in diameter, with lengths ranging from 30 to 40 μm. Both the length and the wall thickness of the nanotubes can be modified by varying the experimental conditions of preparation. XRD measurements show that nanowires are formed by highly textured polycrystals.

According to the literature, La_2O_3 has more applications than $La(OH)_3$, and can be obtained by heating the hydroxide at an adequate temperature. Therefore, the nanotubes prepared here can be used to obtained nanostructured La_2O_3. However, the chemical characterization of the nanotubes reveals that the synthesized material is lanthanum hydroxide partially carbonated. The carbonatation of the samples forces one to increase the decomposition temperature to produce pure La_2O_3.

Acknowledgments

This study has been financed by the Ministry of Education and Science (grant AP2005-2902) and by the Regional Government of Andalusia: Project of Excellence, reference FQM-262; Project of Excellence, reference P06-FQM-02433.

References

[1] Bocchetta P, Santamaria M and Di Quarto F 2007 *Electrochem. Commun.* **9** 683–8
[2] Wang N, Cai Y and Zhang R Q 2008 *Mater. Sci. Eng.* R **60** 1–51
[3] Jayakumar O D, Salunke H G, Kadam R M, Mohapatra M, Yaswat G and Kulshreshtha S K 2006 *Nanotechnology* **17** 1278–85
[4] Kriha O, Zhao L, Pippel E, Gösele U, Wehrspohn R B, Wendorff J H, Steinhart M and Greiner A 2007 *Adv. Funct. Mater.* **17** 1327–32
[5] Tang Y and Ouyang M 2007 *Nat. Mater.* **6** 754–59
[6] Valiev R 2004 *Nat. Mater.* **3** 511–6
[7] Natter H and Hempelmann R 2003 *Electrochim. Acta* **49** 51–61
[8] Xiao R, Cho S, Liu R and Lee S B 2007 *J. Am. Chem. Soc.* **129** 4483–89
[9] Peng Y, Cullis T, Möbus G, Xu X and Inkson B 2007 *Nanotechnology* **18** 485704
[10] Ji C and Searson P C 2003 *J. Phys. Chem.* B **107** 4494–99
[11] Goring P, Pippel E, Hofmeister H, Wehrspohn R B, Steinhart M and Gösele U 2004 *Nano Lett.* **4** 1121–5
[12] Schmid G J 2002 *J. Mater. Chem.* **12** 1231–8
[13] Shi C, Wang G, Zhao N, Du X and Li J 2008 *Chem. Phys. Lett.* **454** 75–9
[14] Zhu W, Wang W, Xu H and Shi J 2006 *Mater. Chem. Phys.* **99** 127–30
[15] Guo Y, Lu G, Zhang Z, Jiang L, Wang X, Li S, Zhang B and Niu J 2007 *Catal. Today* **126** 441–8
[16] Ferrer V, Moronta A, Sánchez J, Solano R, Bernal S and Finol D 2005 *Catal. Today* **107/108** 487–92
[17] Bernal S, Botana F J, García R, Ramírez F and Rodriguez-Izquierdo J M 1987 *J. Mater. Sci.* **22** 3793–800
[18] Helen G and Vishnu P 1999 *Chem. Mater.* **11** 3561–64
[19] Dexpert H and Caro P 1974 *Mater. Res. Bull.* **9** 1577
[20] Sun J, Kyotani T and Tomita A 1986 *J. Solid State Chem.* **65** 94–99
[21] Bernal S, Botana F J, García R and Rodriguez-Izquierdo J M 1983 *Thermochim. Acta* **66** 139–45
[22] Bernal S, Botana F J, García R and Rodriguez-Izquierdo J M 1987 *React. Solids* **4** 23–40
[23] Nagashima K, Wakita H and Mochizuki A 1973 *Bull. Chem. Soc. Japan* **46** 152
[24] Jin C, Xiang X, Jia C, Liu W, Cai W, Yao L and Li X 2004 *J. Phys. Chem.* B **108** 1844–7